Khisina, N. R., Badyukov, D. D., Wirth, R. (2016): Microtexture, nanomineralogy, and local chemistry of cryptocrystalline cosmic spherules. - *Geochemistry International*, *54*, 1, pp. 68—77.

DOI: http://doi.org/10.1134/S0016702916010067

Microtexture, Nanomineralogy, and Local Chemistry of Cryptocrystalline Cosmic Spherules

N. R. Khisina[a], D. D. Badyukov[a], and R. Wirth[b]

[a] *Vernadsky Institute of Geochemistry and Analytical Chemistry, Russian Academy of Sciences, ul. Kosygina 19, Moscow, 119991 Russia*

e-mail: khisina@geokhi.ru

[b] *GeoForschungZentrum Potsdam 14473 Potsdam, Germany*

Received May 20, 2015; in final form, June 29, 2015

Abstract—The paper reports scanning electron microscopy (FEG-SEM) and transmission electron microscopy (TEM) data on three cryptocrystalline (CC) cosmic spherules of chondritic composition (Mg/Si ≈ 1) from two collections taken up at glaciers at the Novaya Zemlya and in the area of the Tunguska event. The spherules show "brickwork" microtextures formed by minute parallel olivine crystals set in glass of pyroxene–plagioclase composition. The bulk-rock silicate chemistry, microtexture, mineralogy, and the chemical composition of the olivine and the local chemistry of the glass in these spherules testify to a chondritic source of the spherules. The solidification of the spherules in the Earth's atmosphere was proved to be a highly unequilibrated process. A metastable state of the material follows, for example, from the occurrence of numerous nanometer-sized SiO_2 globules in the interstitial glass. These globules were formed by liquid immiscibility in the pyroxene–SiO_2 system. Troilite FeS and schreibersite $(Fe,Ni)_3P$ globules were found in the FeNi metal in one of the spherules, which suggests that the precursor was not chemically modified when melted in the Earth's atmosphere. Our results allowed us to estimate the mineralogy of the precursor material and correlate the CC spherules with the chondrule material of chondrites. The bulk compositions of the spherules are closely similar to those of type-IIA chondrules.

Keywords: cosmic dust, micrometeorites, cosmic spherules, chondrites, microtexture, transmission electron microscopy, melting, liquid immiscibility, nanomineralogy

DOI: 10.1134/S0016702916010067

INTRODUCTION

Cosmic spherules (CS) are rounded objects produced by the melting particles of extraterrestrial material when they entered the Earth's atmosphere (Genge et al., 2008). The spherules range from 30 μm to 1–1.5 mm and consist of silicate material, often with magnetite, or are occasionally silicate in composition and contain metal inclusions. Some of the spherules are "iron" and are made up of Ni-bearing magnetite and wustite and often contain Fe–Ni metal cores. A cosmic origin of the spherules follows from their Ni and Ir concentrations (Brownlee et al., 1984), their oxygen isotopic composition (Clayton et al., 1986; Taylor et al., 2005; Yada et al., 2005; Engrand et al., 1998), the presence of taenite and/or kamacite, and from similarities between their composition and those of chondrites (except only very rare eucrite CS). For example, the bulk composition of most of the silicate spherules define a clear-cut compositional trend in the Mg–Fe–Si diagram, with this trend showing a typical "solar" Mg/Si ratio close to 1, which is typical of chondrites. Representative collections of CS were gathered at Antarctic ice cap (Maurette, 1991; Rochette et al., 2008; Taylor et al., 1991, 2000; Yada and Kojima, 2000) and composed by separating the material from oceanic sediments (Brownlee, 1979; Blanchard et al., 1980; Parashar et al., 2010). Cosmic spherules are usually thought to be produced via melting micrometeoroids upon their high-velocity entry in the Earth's atmosphere and deceleration in it (Love and Brownlee, 1991).

The chemical transformation of the precursor at a high-velocity atmospheric entry of the micrometeorite and its collision with gas molecules can be associated with vaporization of volatile (S, P, CO, CH_4, CO_2, H_2O, etc.) and mildly volatile (Fe, Mg, and Si) elements and their compounds and with redox reactions changing the valence of Fe (Brownlee et al., 1997; Taylor et al., 2005; Cordier et al., 2011). In interpreting data on the composition of cosmic spherules, it is important to understand as to how much the chemical composition of the spherules and variations in this composition reflect the chemistry of the solid precursors (micrometeorites) and how much the compositional variations may be indicative of changes in the composition of the solid precursors during their melting in the Earth's atmosphere.

According to the type of their microstructures, silicate CS (Fig. 1) are classified into porphyritic (PO), barred (BO), cryprocrystalline (CC), and glassy (GS) (Blanchard et al., 1980). The heating temperature due

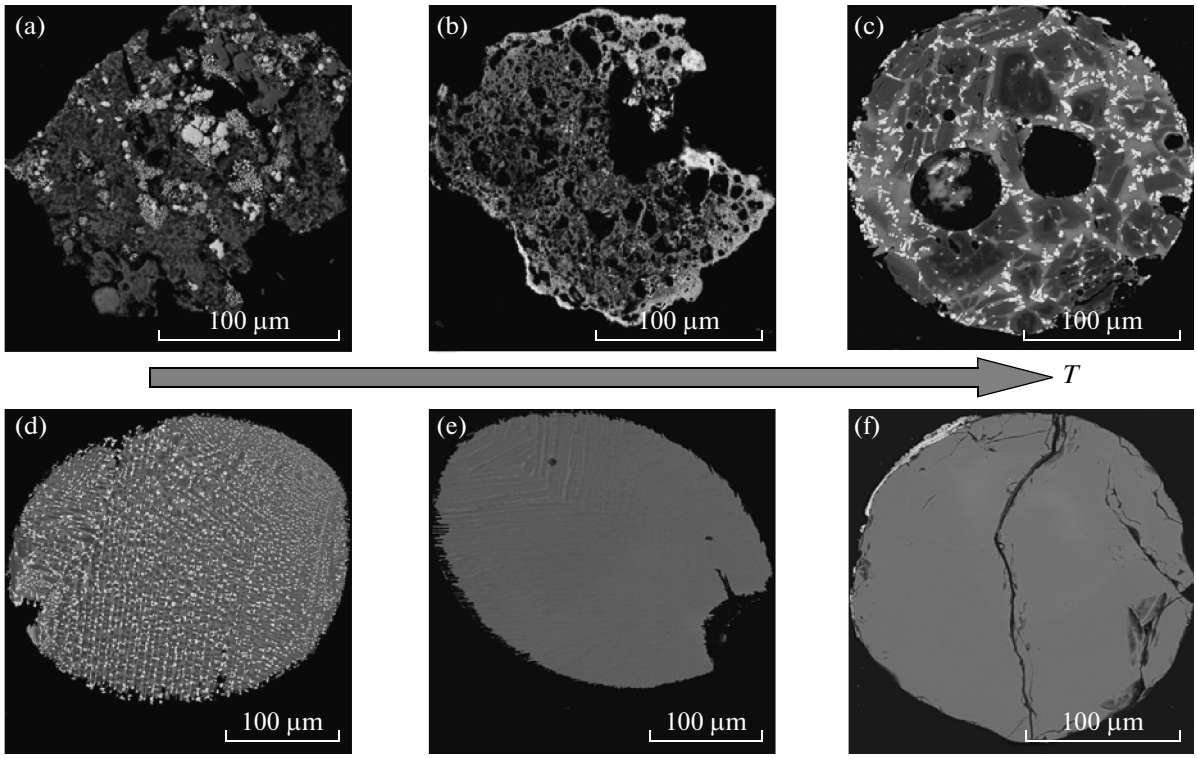

Fig. 1. BSE images of polished sections of various types of micrometeorites. (a) Unmelted micrometeorite; (b) partly melted (scoriaceous) micrometeorite; (c–f) melted micrometeorites—cosmic spherules of major microtextural types: (c) porphyritic spherule, (d) olivine spherule, (e) cryptocrystalline spherule, (f) glass spherule. The heating temperature of the micrometeorites increased from (a) to (f), as indicated by the arrow, when the micrometeorites passed through the Earth's atmosphere, and correspondingly increased the extent of micrometeorite transformations.

to micrometeorite deceleration in the atmosphere increases from PO to GS. The cryptocrystalline spherules are ovoid and/or spindly in shape and are made up of submicrometer-sized crystallites set in a glass matrix. They compose approximately 12% of the total number of silicate spherules in SPWW of the Antarctic collection (Taylor et al., 2000). The microtexture, mineralogy, and local chemistry of the silicate material of the cryptocrystalline spherules containing crystallites that cannot be examined by SEM due to their small size are studied still much more poorly than those in the spherules of other types.

This publication presents our SEM and TEM data on three cryptocrystalline (CC) cosmic spherules of chondritic composition (Mg/Si ≈ 1) from two collections taken up in the ice cap of the Novaya Zemlya (Badjukov and Raitala, 2003) and separated from soil samples from the area of the Tunuska event (Badyukov et al., 2011).

MATERIALS AND METHODS

Cosmic spherules from the Novaya Zemlya Archipelago were collected in the marginal part of the Novaya Zemlya ice cap (Badjukov and Raitala, 2003; Badjukov et al., 2010). Samples of solid sediment on ice (cryoconite) were washed to get rid of the clay constituent and subjected to magnetic separation. The Tunguska material was collected by A.V. Ivanov in 1960 via separating spherules from the uppermost soil layer in the terrace above the flood-plain of the Chunya River near the epicentrum of the Tunguska event (Badyukov et al., 2011).

The CS were hand-picked from the enriched samples under a binocular microscope to prepare polished sections with CS. The polished sections were then examined under a JEOL JSM 6400 analytical scanning electron microscope and JEOL JXA-8200 X-ray microprobe at the University of Oulu in Finland. The bulk composition of the spherules was analyzed by SEM equipped with an EDS via scanning selected areas and via local microprobe analyses at 15 kV accelerating voltage and 10 nA beam current. In the latter instance, a beam defocused to 20 μm in diameter was employed, and each spherule was analyzed at three to six spots. The analyzer was calibrated on certified elemental, oxide, and silicate standard reference samples, with the date corrected using the ZAF JEOL proprietary software. Major elements were analyzed accurate to ~2% at a detection threshold of 0.02 wt %.

The material selected for our TEM study was three cryptocrystalline spherules: two from Novaya Zemlya (spherules NZ8-bn4-25,9 and bn3-3-40) and one from the Tunguska area (spherule T3-2). A metal droplet-

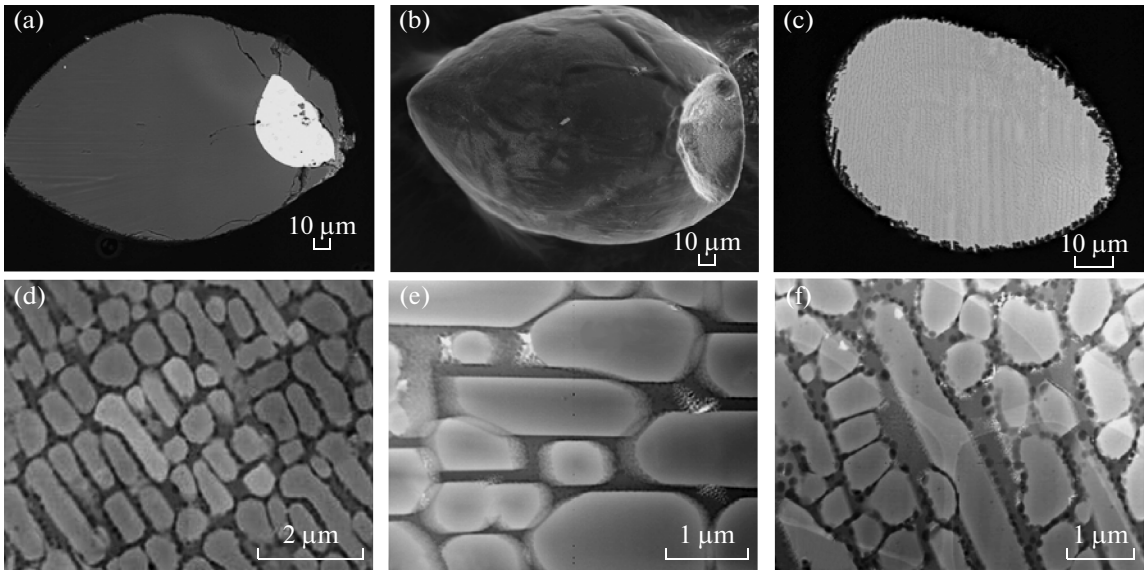

Fig. 2. Cryptocrystalline spherules from the Novaya Zemlya and Tunguska area. (a) Spherule T3-2 (Tunguska); (b, c) spherules NZ8-bn4-25,9 and bn3-3-40 (Novaya Zemlya). The images display a partly preserved FeNi metal droplet in spherule T3-2 (Fig. 2a), a pit left by a lost droplet on the surface of solid phase NZ8-bn4-25,9 (Fig. 2b), and the absence of both metal inclusions and evidence of their loss in spherule bn3-3-40 (Fig. 2c). The spherules have "brickwork" microtextures defined by similarly oriented olivine crystals in glass.

shaped incomplete sphere approximately 60 μm in diameter (Fig. 2a) was detected on the surface of spherule T3-2. A pit on the surface of spherule NZ8-bn4-25,9 has a shape of hemisphere and does not contain any metal (Fig. 2b). Spherule bn3-3-40 is free of metal, and its surface has no concave pits (Fig. 2c). Our TEM samples were prepared in the form of FIB foil cut out of the thin section perpendicular to its plane or to the spherule surface. The study was carried out at the GeoForschungZentrum in Potsdam, Germany, at an accelerating voltage of 200 kV at a TECNAI F20 XT equipped with a field emission gun (FEG), high-angle annular dark field (HAADF) detector, energy dispersive analyzer of X-ray (EDAX), and a Gatan imaging filter (GIF) Tridiem. The technical potentialities of the equipment make it possible to obtain bright-field (BF), dark-field (DF), bright-field/dark-field (BFDF), and high-angle annular (HAADF) images; to conduct chemical analyses at spots and via scanning; to shoot concentration profiles and carry out elemental mapping; and to obtain high-resolution electron-diffraction imagery.

RESULTS

The spherules are ellipsoidal or spindle-shaped (Fig. 2), and their sizes are ≈130 × 200 μm (spherule T3-2), ~100 μm (spherule NZ8-bn4-25,9), and ~50 × 70 μm (spherule bn3-3-40). The bulk chemical compositions of spherules T3-2 and bn3-3-40 are reported in Table 1, and spherule NZ8-bn4-25,9 has not been studied by either microprobe and SEM techniques and its bulk composition was not determined.

The three cryprocrystalline spherules have brickwork-type structures, which are formed by similarly oriented olivine crystals in silica-rich glass of pyroxene–plagioclase composition (Fig. 2). The size of the olivine crystals is ~0.5 × 1.5 μm (spherule T3-2), ~0.9 × 2 μm (spherule NZ8-bn4-25,9), and ~0.7 × 4.5 μm (spherule bn3-3-40). The olivine crystals (of roughly equal size) are elongate along [010], subparallel to one another within the spherule, and thus form brickwork-resembling structures (with "brick" rows parallel to [010] of the olivine crystals) set in glass. The crystals are rounded in cross section. The spherules contain 60–70 vol % olivine. The interstitial glass between olivine crystals abounds in variably sized globules approximately 100 nm across (Figs. 3a, 3b), whose composition corresponds to almost pure SiO_2 (Fig. 3c). The SiO_2 globules decorate the faces of olivine crystals and make them look like corroded. Along with SiO_2 globules, the glass contains chromite dendrites (Fig. 4). In spherule bn3-3-40, vermicular aggregates of nanometer-sized chromite occur in glass at boundaries of olivine crystals. In spherules T3-2 and CS NZ8-bn4-25,9, chromite has never been found in contact with olivine, and chromite aggregates are hosted in glass of plagioclase composition (Fig. 4).

The chemical composition of the olivine and interstitial glass of the spherules is shown in Table 1. The olivine is merely weakly zoned: $Fo_{70–76}$. The interstitial glass is of pyroxene–plagioclase composition, but contains excess SiO_2 relative to this system. The chemical composition of olivine and interstitial glass and the bulk composition of spherule bn3-3-40, recalculated to

Table 1. Microprobe analyses (at %) of spherules and TEM-EDS analyses (at %) of olivine and interstitial glass

Element	Olivine				Glass			Bulk composition	
	Bn3-3-40		T3-2		NZ8-bn4-25,9		Bn3-3-40	T3-2	Bn3-3-40
	1*	2*	1*	2*					
Mg	54.4	50.5	51.1	49.8	8.0	6.0	7.4	40.25	34.65
Si	30.9	32.5	34.7	34.4	55.9	60.1	57.7	43.45	44.18
Cr	0.5	0.2	0.3	0.1	bdl	bdl	0.1	0.39	0.29
Mn	0.2	0.3	0.4	0.2	0.1	0.2	0.7	0.15	0.58
Fe	13.9	16.5	13.6	15.4	14.4	11.8	15.3	11.88	17.47
Ni	bdl	bdl	bdl	bdl	bdl	bdl	bdl	bdl	0.19
Al	bdl	bdl	bdl	bdl	12.2	12.6	11.1	2.27	0.71
Ca	bdl	bdl	bdl	bdl	9.5	8.9	7.5	1.55	1.86

(1*) Analysis of crystal core, (2*) analysis of crystal margin, bdl means concentrations below the detection limits.

atomic percentage after deducing the plagioclase–wollastonite composition, are plotted in the ternary Mg–Fe–Si diagram (Fig. 5). Lines with arrowheads show the chemical separation in the glass with SiO_2 exsolution. The composition of the "pyroxene" glass component complementary to SiO_2 lies on the continuation of the SiO_2 –Glass tie line toward the En–Fs join, as indicated by an arrow in Fig. 5. It is difficult to accurately enough analyze the "pyroxene" component of the glass because of the presence of numerous SiO_2 globules, which may be involved in the analysis.

The droplet-shaped metal phase on the surface of spherule T3-2 has the composition of kamacite $Fe_{0.894}Ni_{0.103}$. BSE images of this thin section show that the kamacite contains ovoid inclusions approximately 3 μm across (Fig. 6a). The inclusions contain Fe, Ni, S, and P. The compositional mapping, spot analyses, and compositional profiling on TEM reveal the complicated compositional heterogeneity of the ovoid inclusions. They consist of a spherical cores (0.75 μm in diameter), which contain Fe, Ni, and S (Fig. 6b), and outer rims, which contain Fe, Ni, and P (Fig. 6c), suggesting that the material consists of two phases. Chemical analyses testify that the cores of the inclusions are made up of a practically exactly equimolar mixture of troilite FeS and Fe–Ni alloy of taenite $Fe_{0.81}Ni_{0.19}$ composition. The phosphide rims are composed of eutectic mixture of nanometer-sized phases of schreibersite $(Fe, Ni)_3P$ and Fe–Ni alloy. The boundary between the core and rim and between the rim and the host kamacite matrix are clearly distinguishable in P and S concentration profiles. The proportion of the phosphide and metal phases in the phosphide rim systematically varies, thus suggesting an increase in the P concentration and decrease in that of Ni from the inner to outer boundaries of the rim (Table 2).

DISCUSSION

Mineralogical Precursors and Unequilibrated Crystallization in the Spherules

The bulk compositions of the cryptocrystalline spherules minus the plagioclase–wollastonite component plot within the stability field of the olivine + pyroxene phase association. Data on the inner structure of the spherules and the chemical composition of their interstitial glass suggest that crystallization in the course of solidification of the spherules was a highly unequilibrated process. An unequilibrated character of olivine crystallization follows from the following chemical, phase, and structural features of the spherules: (1) the absence of pyroxene and a volumetric proportion of olivine (~70%) to glass corresponding to a normative olivine/glass ratio of approximately 2 : 1 (while equilibrium olivine and pyroxene association at this bulk composition corresponds to a normative olivine/pyroxene ratio of ~0.45); (2) the absence of pyroxene in the crystallization products, the silica-rich composition of the glass with atomic ratios $Si/(Mg + Fe) > 1$; (3) numerous nanometer-sized SiO_2 globules in the glass; and (4) a high Mg partition coefficient between the olivine and

Table 2. TEM EDS analyses (at %) of Fe–Ni–S–P inclusions in a FeNi metallic droplet (spherule T3-2)

Element	Metal	Inclusion		
		Core	Margin	
			1*	2*
Fe	89.6	60.6	70.4	66.0
Ni	10.4	6.5	19.3	14.2
S	bdl	32.9	bdl	bdl
P	bdl	bdl	10.3	19.8

(1*) Analysis near the boundary of inclusion margin and its sulfide core, (2*) analysis near the boundary of inclusion margin and host metal, bdl means concentrations below the detection limits.

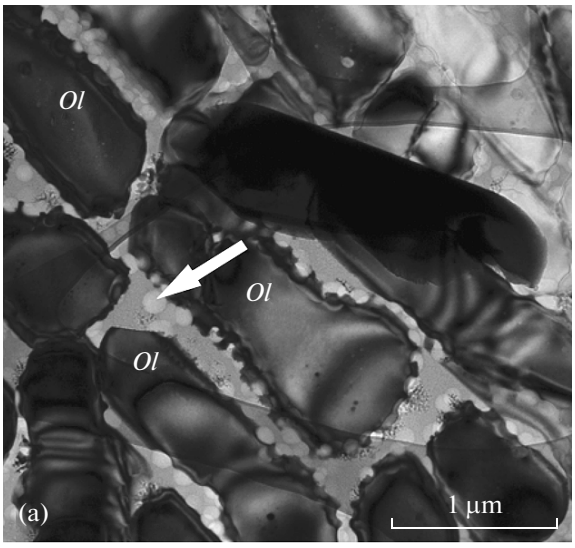

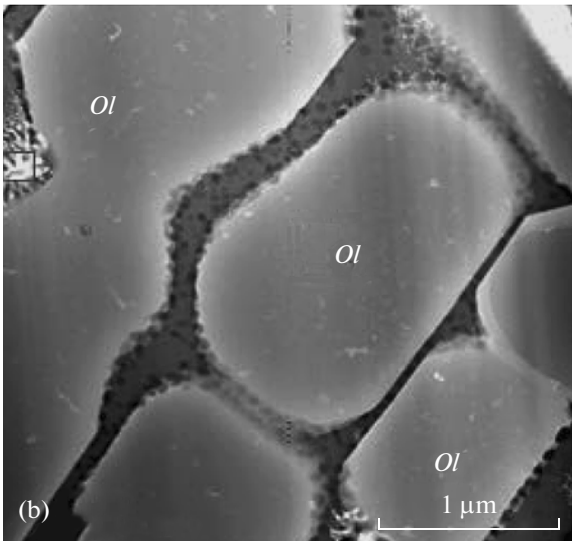

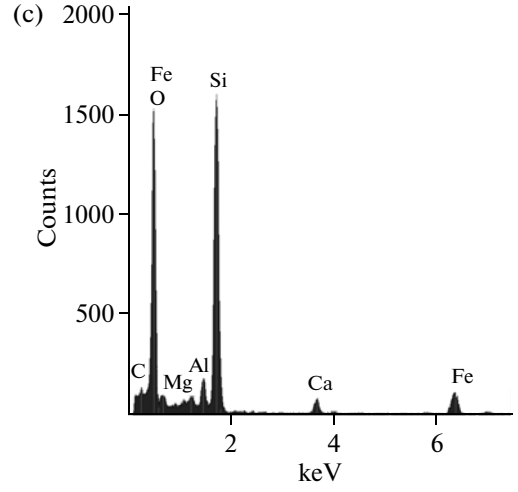

Fig. 3. Nanometer-sized SiO_2 globules (the arrow indicates one of them) at the boundary between olivine and pyroxene–plagioclase glass in spherules (a) bn3-3-40 and (b) NZ8-bn4-25,9. Fig. 3a is an HAADF image, Fig. 3b is a BF image, and Fig. 3c is the EDS spectrum of the SiO_2 globule.

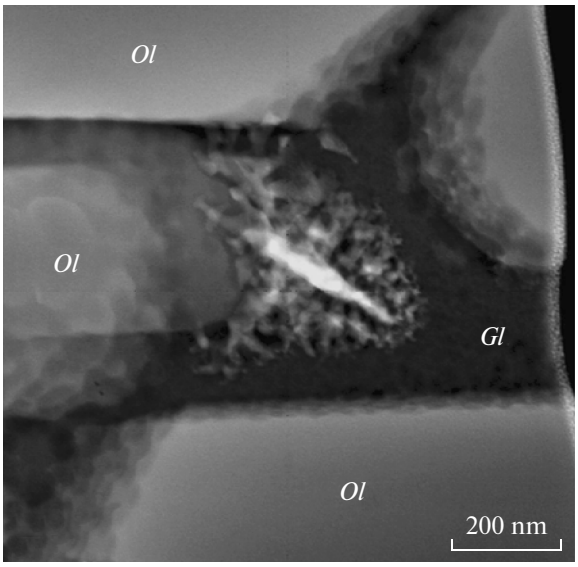

Fig. 4. Chromite aggregate (white) in glass (*Gl*) of plagioclase composition between olivine (*Ol*) crystals. Spherule NZ8-bn4-25,9.

glass: $Mg_{Ol} : Mg_{Gl} = 6.3$. These features should have been predetermined, first of all, by high cooling rates of the melt during passage through the Earth's atmosphere. Note that the porphyritic and barred microtextures of the spherules were reproduced in experiments by cooling melt droplets during times spans of a few seconds (Gondo and Isobe, 2013). The cryptocrystalline spherules should have been produced at even faster cooling. At this very rapid quenching, olivine forms the cryptocrystalline structure of the spherules, and pyroxene has not enough time to crystallize. Experiments in the $MgO–SiO_2$ system (Kirkpatrick et al., 1983) have demonstrated that melt containing 59 wt % SiO_2 can crystallize only olivine even at relatively low cooling rates of 0.4–25°/min, and no pyroxene nucleates. The behavior of the system is defined as metastable crystallization from supercooled melt. Quenching explains the volumetric proportions of olivine and glass in the spherules, which seem to indicate that olivine continued to crystallize in the stability field of pyroxene $a\mathrm{Ol} + bPx \rightarrow$ melting $\rightarrow \rightarrow$ solidification $\rightarrow [(a + x)\mathrm{Ol}]$crystal + $[(b - 2x)Px + x\mathrm{SiO_2}]$glass. Nanometer-sized SiO_2 globules in the interstitial glass of the spherules (Fig. 3) were produced by nanometer-scale liquid immiscibility and testify to the well-known phenomenon of liquid immiscibility in the $Px–SiO_2$ system (Chen and Presnall, 1975). Liquid immiscibility in oxide and silicate glasses was observed in oxide and silicate glasses produced by melt quenching at temperatures below the binodal and spinodal (Galakhov, 1964; Andreev et al., 1974; Kirillova et al., 2012; Veksler et al., 2008).

The $Mg_2SiO_4–SiO_2$ equilibrium melting diagram involves peritectic and eutectic points (Fig. 7). The melting of pyroxene is incongruent according to the

peritectic reaction pyroxene = olivine + $(Px + SiO_2)_{pmelt}$ (Chen and Presnall, 1975; Dalton and Presnall, 1997; Kirkpatrick et al., 1983). In the high-temperature region of the right-hand part of the olivine–SiO_2 diagram, a dome of liquid immiscibly (binodal) occurs between pyroxene and SiO_2 (Fig. 7).

Note that the equilibrium crystallization of Fe–Mg olivine–pyroxene melt at decreasing temperature produces olivine, and the composition of the equilibrium melt is thereby enriched in Fe and SiO_2. Olivine crystallization terminates when the peritectic temperature is reached, with high-Fe pyroxene starting to crystallize below it, and the melt continuing to enrich in SiO_2. As the temperature decreases, olivine partly dissolves, reacts with the residual melt, and forms pyroxene. The solidification process terminates at the eutectic point with the origin of the olivine + pyroxene two-phase association.

Considering the scenario of metastable behavior of the system (Fig. 7), we assume that the olivine liquidus can has a metastable continuation, as also do the binodal and spinodal curves of liquid immiscibility, in the low-temperature region of the olivine–SiO_2 diagram. [1] In so doing, we proceed from the assumption that crystallizing olivine does not interact with the coexisting melt. When the metastable continuations of the liquidus curve and binodal intersect (Fig. 7, point *A*) or when the liquidus curves intersect the spidodal (Fig. 7, point *B*), the melt starts to break down into two immiscible liquids, one of which is enriched and the other is depleted in silica. Further cooling is associated with a systematic change in the bulk composition of the melt along the liquidus curve, with metastable olivine crystallization continuing in the melt that undergoes liquid immiscibility. The metastable olivine crystallization in the melt terminates at point *C* at T_{Gl}, which is the vitrification temperature of the melt that has exsolved into two liquids of the composition *D* and *E*. The *BCD* region of the metastable diagram is characterized by the coexistence of olivine and two liquids. Chemical analyses of spherule bn3-3-40 (Table 1) allowed us to plot the bulk compositions of the spherule (I) and glass (II) in the phase diagram of the olivine–SiO_2 system (Fig. 7). The point of the experimentally determined composition of the glass at the temperature T_{Gl} plots within the liquid immiscibility field (Fig. 7, point *C*). The occurrence of SiO_2 in the form of isolated nanometer-sized globules in the glass of the spherules corresponds to the morphology typical of the metastable transformation according to *spinodal* but not *binodal* decomposition (Galakhov, 1964; Andreev et al., 1974). This means that the onset of chemical exsolution of the residual melt during its solidification is determined by point *B* of the intersection of the metastable continuation of the liquidus curve and spinodal. In the phase diagram, the spinodal curve has a region of metastable liquid immiscibility. At quenching, the onset of liquid immiscibility is realized according to a spinodal but not binodal mechanism, because the activation energy of spinodal transformation is lower and this process has a higher rate.

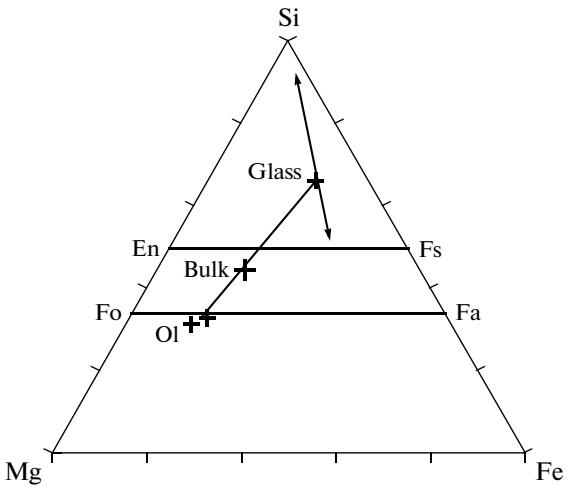

Fig. 5. Chemical compositions (at %) of olivine (*Ol*) and glass (*Gl*) and the bulk composition of spherule (Bulk) bn3-3-40. Arrows indicate the liquid-immiscibility exsolution trends of the glass into compositions close to SiO_2 and pyroxene.

The nanomineralogy, structural features, and local chemistry of the glass in the cryptocrystalline spherules thus reflect unequilibrated solidification of olivine–pyroxene mineralogical precursors of the spherules that were melted in the Earth's atmosphere.

Origin of FeNi Metal in the Cryptocrystalline Spherules

According to (Taylor et al., 2000), 32% of the cryptocrystalline spherules contain FeNi or FeS droplets. Each of the spherules usually hosts a single metal droplet, which is spherical and occurs not at the center of the spherule but closer to its surface, being displaced there by inertia when the melted micrometeoroid passed through the Earth's atmosphere (Brownlee et al., 1984; Genge and Grady, 1998). Moving of the metallic droplet toward a surface in the spherule was associated with the partial (Fig. 2a) or complete metal removal from the spherule, which then left a pit on the surface of the spherule (Fig. 2b). Six of our fourteen cryptocrystalline spherules from Novaya Zemlya bear hemispherical pits on their surfaces (Fig. 2a), one of the spherules contains a partly preserved FeNi droplet on, and seven spherules do not posses either pits or metal at all.

The FeNi metal droplets in the spherules can be of primary (cosmic) origin, thus testifying that FeNi was contained in the precursor material. However, the FeNi

[1] Note that this diagram of metastable crystallization (Fig. 7) is based on the Mg_2SiO_4–SiO_2 equilibrium phase diagram in which the possible presence of Fe, Ca, and Al (Table 1) silicate material is ignored, although these elements should shift the boundaries of phase equilibria.

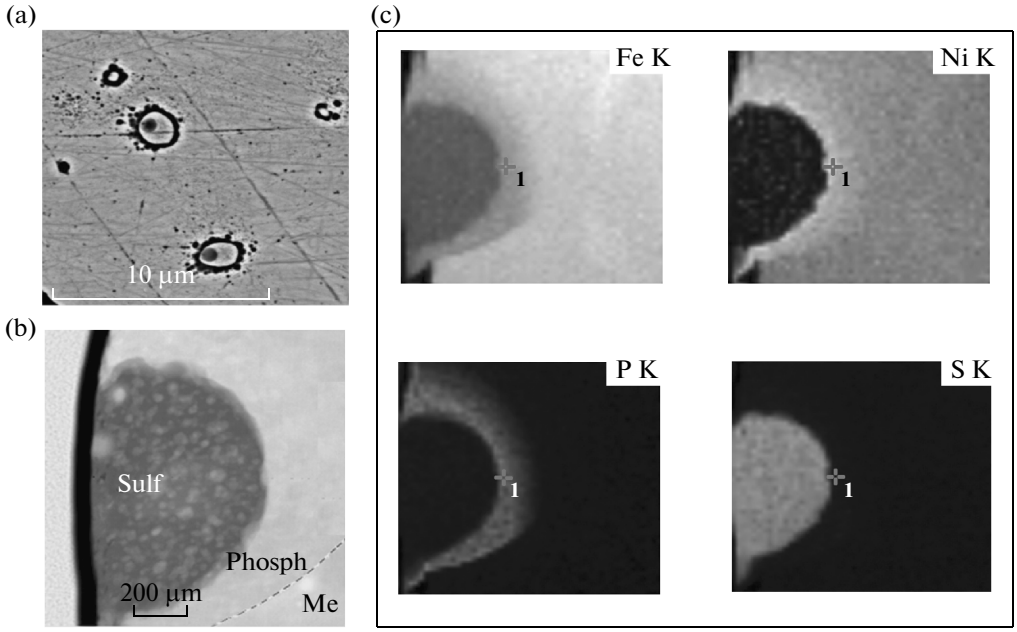

Fig. 6. Ovoid inclusion in a FeNi metal droplet (spherule T3-2). (a) BSE-SEM image of the thin section; black "rims" around inclusions are caused by spalling in the process of polishing; (b) TEM image of an inclusion in a FIB film cut off the thin section perpendicular to its surface (*Sulf* is the sulfide core, *Phosph* is the phosphide rim, and *Me* is the host FeNi metal); (c) is a Fe, NI, P, and S element-concentration map of the inclusion.

droplets might also be of secondary nature and be produced in the spherules via the reduction of these elements in silicates when the micrometeoroid flew through the upper rarefied atmospheric layers of the Earth (Brownlee et al., 1997; Taylor et al., 2005). This hypothesis is underlain by the fact that the cryptocrystalline and barred spherules have the same Mg/Si ≈ 1, but the material of the former often hosts metal droplets and is richer in Fe than that of the barred spherules, which typically bear no metal. Hypothesizing that the material of both the cryptocrystalline and the barred spherules originated from the same source, some researchers (Brownlee et al., 1984, 1997; Taylor et al., 2005) argue that the relative Fe depletion of the silicate constituent of the cryptocrystalline spherules and the origin of metal in them can be explained by Fe^{2+} (and Ni^{2+}) removal from the silicate melt by reduction reactions. The possible metal-forming reactions were suggested to be reduction with carbon in the form of graphite $FeO + C = Fe^0 + CO\uparrow$, impact S vaporization $FeS = Fe^0 + S\uparrow$, and pyrolysis of the carbonaceous matter of chondrites (Brownlee et al., 1984, 1997; Taylor et al., 2005).

Our data rule out a secondary nature of FeNi metal in spherule T3-2 and argue for pristine, i.e., cosmic, origin of FeNi droplets in the cryptocrystalline cosmic spherules. The origin of the FeNi droplets via reduction of oxides is in contradiction with the fact that the glasses of the spherules host chromite (Fig. 4), which suggests that Cr occurred in the melt in the form of Cr^{3+}. The $Fe^{2+} \rightarrow Fe^0$ and $Ni^{2+} \rightarrow Ni^0$ reactions of oxide reduction can proceed at $\log fO_2 \leq$ IW (Berry and O'Neil, 2004), whereas Cr^{3+} can occur in melt at an oxygen fugacity of IW + 5 > $\log fO_2$ > IW (Berry et al., 2004). It is also worth mentioning that the chemical composition of the silicate constituent of spherule T3-2, which contains a metal droplet, is closely similar to that of spherule bn3-3-40, which does not contain metal and shows no evidence that the metal droplet could have been lost when passing through the atmosphere. Had the metals been reduced from oxides originally contained in the silicate melt, the bulk compositions of these spherules would have contained remarkably different Fe concentrations in the silicate material: the silicate material of spherule T3-2 would have been poorer in Fe than that of spherule bn3-3-40. A convincing argument in favor of a pristine nature of the metal is furnished by the occurrence of troilite–schreibersite globules in the FeNi metal droplet in spherule T3-2 (Fig. 6). Schreibersite $(Fe, Ni)_3P$ and troilite FeS are typical cosmic minerals of inclusions in FeNi metal of iron meteorites, but they cannot be formed as inclusions in metal during the reduction of Fe and Ni oxides in silicate melt.

Transformations of the Precursor Material upon Its Atmospheric Entry

The arguments presented above led us to conclude that that material of the precursors of the cryptocrystalline spherules has not undergo transformation in the Earth's atmosphere that were associated with the

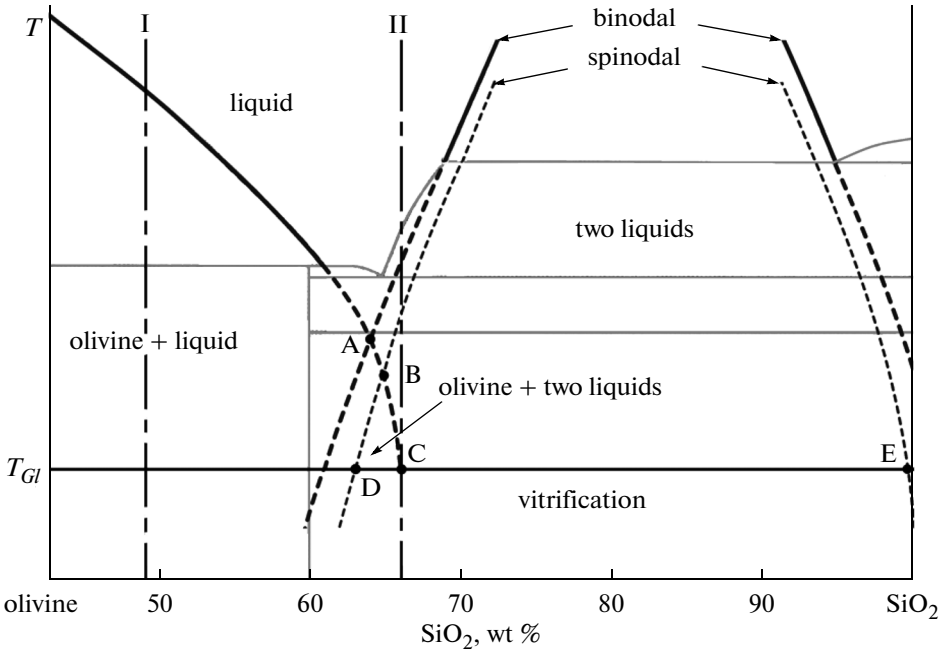

Fig. 7. Schematic phase diagram of unequilibrated olivine crystallization, based on data on the Mg_2SiO_4–SiO_2 system (Kirkpatrick et al., 1983). Solid black and gray lines show equilibrium phase boundaries. Dashed lines show metastable continuations of the olivine liquidus and binodal constraining the liquid immiscibility region and the spinodal. T_{Gl} is the vitrification temperature, I is the bulk composition of spherule bn3-3-40, II is the bulk composition of glass in this spherule. See text for explanations of the symbols *A, B, C, D*, and *E*.

reduction of Fe (and Ni) to their metallic state. Indicators of conditions ruling out the reduction reactions $Fe^{2+} \rightarrow Fe^0$ and $Ni^{2+} \rightarrow Ni^0$ in the melt are chromite contained in the glass (Fig. 4) and troilite–schreibersite inclusions in the FeNi metal (Fig. 6).

Troilite–schreibersite globules in a droplet of FeNi metal in spherule T3-2 suggest not only that the FeNi metal is of pristine nature but also that neither S nor P vaporized in the course of precursor melting. Correspondingly, we also rule out and possibility that less volatile elements (Fe, Si, and Mg) could then vaporize. This is consistent with conclusions derived from the oxygen isotopic composition of the porphyritic and barred spherules (Yada et al., 2005; Engrand et al., 1998). According to these authors, variations in the oxygen isotopic composition of the spherules reflect the variations in the oxygen isotopic composition of the precursors and did not result from oxygen vaporization in the Earth's atmosphere.

It is worth mentioning that the conclusion that oxygen did not vaporize is consistent with the above conclusion that neither iron nor nickel were reduced from their oxides to metals in the course of atmospheric melting. The conclusion that neither sulfur for phosphorus are vaporized is, in turn, consistent with the conclusion that the FeNi metal of the spherules could not been produced by the reduction of sulfides to metallic Fe^0 and Ni^0.

The aforementioned data and arguments based on them led us to conclude that the material of the precursors of the cryptocrystalline spherules has not been modified in the Earth's atmosphere, and the chemical composition of the spherules thus corresponds to the chemical composition of their solid precursors.

Correlations between the Material of the Spherules and Types of Chondritic Material

It is currently believed that the solid precursors of the cosmic spherules (micrometeoroids) were produced by the disintegration of the rocks of asteroidal or cometary bodies during their collisions in space. The sizes of both remelted and unremelted micrometeorites (CS) are tens to hundreds of micrometers. The bulk composition of such small particles obviously cannot be representative enough to be compared with the bulk composition of coarse-crystalline differentiated material of the parent bodies, such as achondrites. The presence of achondritic material (the coarse-crystalline fabric of the precursor) can explain the variations in the CS (melting products of micrometeorites) in terms of Mg, Fe, and Si concentrations in the Fo–Fa–Fs–En compositional field. At the same time, most silicate CS posses Mg/Si atomic ratios close to one, which corresponds to the "solar composition" of the most primitive (undifferentiated) material of the Solar System. Representative fragments of the primitive material produced very early during the origin of the Solar System are carbonaceous

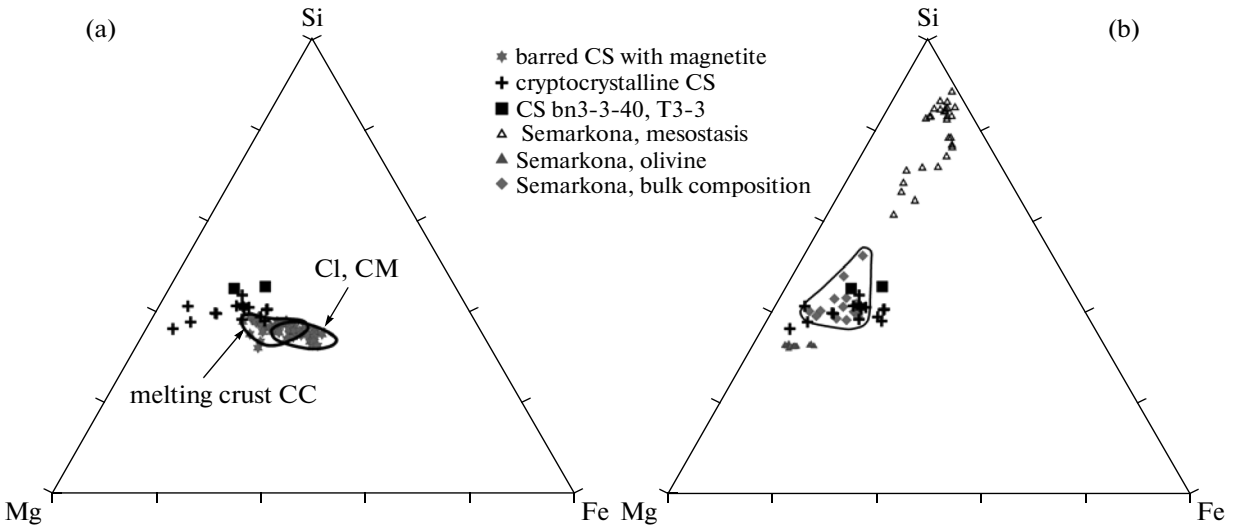

Fig. 8. Comparison of the bulk compositions of (a) cryptocrystalline an barred cosmic spherules (CS) in comparison with CI and CM carbonaceous chondrites and the melting crust of carbonaceous chondrites (the diagram shows the bulk compositions of spherules from the Novaya Zemlya and the points of the bulk compositions of spherules bn3-3-40 and T3-2; compositional regions of CI and CM chondrites and the melting crust of carbonaceous chondrites are contoured); (b) cryptocrystalline cosmic spherule (from the Novaya Zemlya) and chondrules of the Semarkona meteorite (Hewins et al., 2012) (the field of the bulk compositions of chondrules is contoured; the composition of the mesostasis and olivine in the chondrules are complementary).

chondrites, which consist of a fine-grained matrix (which is dominated by phyllosilicates, first of all, serpentine and other components) and chondrules (which have a mostly olivine composition and are up to a few millimeters in diameter). The chemical compositions of chondrules and matrixes are complementary (Hewins et al., 2012; Palme et al., 2015), and the regions of the bulk compositions of carbonaceous chondrites in the Mg–Fe–Si ternary diagram plot around the line of an atomic ratio Mg/Si = 1 (Fig. 8a). Currently available extensive data show that hydrous interplanetary dust particles (IDPs) and fine-grained unmelted micrometeorites show mineralogical and chemical similarities with the fine-grained matrix of carbonaceous chondrites (Kurat et al., 1994; Genge et al., 1997). Cosmic spherules whose precursor was the fine-crystalline material of carbonaceous chondrites should also largely retain chemical features of the material of carbonaceous chondrites with an atomic ratio Mg/Si ≈ 1. Indeed, the composition field of barred spherules overlaps the field of carbonaceous chondrites (Fig. 8a) and defines a clearly pronounced trend with Mg/Si ≈ 1 in the Mg–Fe–Si diagram at Fe/Mg varying from 1.0 to 0.25. Data on oxygen isotopic fractionation make it possible to parallel the material of BO spherules with various types of carbonaceous chondrites (Yada et al., 2005; Clayton et al., 1986; Taylor et al., 2005; Engrand et al., 1998).

However, the bulk composition of the cryptocrystalline spherules has Fe/Mg ≤ 0.25 and plots outside the bulk composition field of carbonaceous chondrites (Fig. 8a). The bulk compositions of spherules T3-2 and bn3-3-40 do not correspond to either the bulk composition of the matrix or that of chondrules of carbonaceous chondrites. At the same time, the bulk compositions of cryptocrystalline spherules T3-2 and bn3-3-40 are closely similar to the bulk compositions of chondrules of the Smarkona LL3.0 ordinary chondrite (Fig. 8b). According to the currently adopted chemical systematics of chondrules (Jones, 1990; Lauretta et al., 2006), chondrules in the Smarkona are classed with Fe-rich chondrules of type IIA. Analogies between the bulk composition of olivine–pyroxene chondrules in meteorites and several cosmic spherules of various microstructural types were emphasized in some earlier publications (Taylor et al., 2005; Engrand et al., 1998). Our data on the analogy between the chemical composition of the chondrules of ordinary chondrites and cryptocrystalline cosmic spherules collected in widely spaced areas (Novaya Zemlya and the basin of the Tunguska River) led us to suggest that individual chondrules could be typical enough solid precursors of cosmic spherules.

ACKNOWLEDGMENTS

The authors thank I.V. Veksler for help and valuable consultations during the preparation of the manuscript. A.A. Kadik, O.A. Lukanin, and M.A. Nazarov are thanked for assistance and discussions of our results.

REFERENCES

N. S. Andreev, O. V. Mazurin, E. A. Porai-Koshits, G. P. Roslova, and V. N. Filippovich, *Liquid Immiscibility in Glasses*, (Nauka, Leningrad, 1974) [in Russian].

D. D. Badjukov and J. Raitala, "Micrometeorites from the northern ice cap of the Novaya Zemlya archipelago, Russia:

the first occurrence," Meteorit. Planet. Sci. **38**, 329–340 (2003).

D. D. Badjukov, F. Brandstätter, J. Raitala, and G. Kurat, "Basaltic micrometeorites from the Novaya Zemlya glacier," Meteorit. Planet. Sci. **45** (9), 1502–1512 (2010).

D. D. Badjukov, A. V. Ivanov, J. Raitala, and N. R. Khisina, "Spherules from the Tunguska event site: could they originate from the Tunguska cosmic body?" Geochem. Int. **49** (7), 641–653 (2011).

A. J. Berry and H. St. O'Neill, "A XANES determination of the oxidation state of chromium in silicate glasses," Am. Mineral. **89**, 790–798 (2004)

M. B. Blanchard, D. E. Brownlee, T. E. Bunch, P. W. Hodge, and F. T. Kyte, "Meteoroid ablation spheres from deep sea sediments," Earth Planet. Sci. Lett. **46**, 178–190 (1980).

D. E. Brownlee, B. A. Bates, and R. H. Beauchamps, "Meteor ablation spherules as chondrule analogs," in *Chondrules and their Origin*, Ed. by E. A. King (Lunar and Planetary Institute, Houston, 1984), pp. 10–25.

D. E. Brownlee, B. Bates, and L. Schram, "The elemental composition of stony cosmic spherules," Meteorit. Planet. Sci. **32**, 157–175 (1997).

D. E. Brownlee, L. B. Pilachowski, and P. W. Hodge, "Meteorite mining in the ocean floor," Lunar Planet. Sci. Conf. **10**, 109–111 (1979).

C.-H. Chen and D. C. Presnall, "The system Mg_2SiO_4–SiO_2 at pressures up to 25 kilobars," Am. Mineral. **60**, 398–406 (1975).

R. N. Clayton, T. K. Mayeda, and D. E. Brownlee, "Oxygen isotopes in deep-sea spherules," Earth Planet. Sci. Lett. **79**, 235–240 (1986).

C. Cordier, L. Folco, C. Suavet, C. Sonzogni, and P. Rochette, "Major, trace element and oxygen isotope study of glass cosmic spherules of chondrite composition: the record of their source material and atmospheric entry heating," Geochim. Cosmochim. Acta **75**, 5203–5218 (2011).

J. A. Dalton and D.C. Presnall "No liquid immiscibility in the system $MgSiO_3$–SiO_2 at 5.0 GPa," Geochim. Cosmochim. Acta **61** (12), 2367–2373 (1997).

C. Engrand, K. D. McKegan, L. A. Leshin, and D. E. Brownlee, "In-situ measurement of oxygen isotopic compositions of deep-sea and Antarctic cosmic spherules," Lunar Planet. Sci. Conf. **29**, abstract #1473 (1998).

F. Ya. Galakhov, "Microliquid immiscibility and its image in the two-phase diagram," Izv. Akad. Nauk, Ser. Khim., No. 8, 1377–1383 (1964).

M. J. Genge and M. M. Grady, "Melted micrometeorites from Antarctic ice with evidence for the separation of immiscible Fe–Ni–S liquids during entry heating," Meteorit. Planet. Sci. **33**, 425–439 (1998).

T. Gondo and H. Isobe, "Artificial cosmic spherules produced by melting experiments of the powdered Allende meteorite,' Lunar Planet. Sci. Conf. **44**, abstract #1882 (2013).

R. H. Hewins, B. Zanda, and C. Bendersky, "Evaporation and recondensation of sodium in Semarcona Type II chondrules," Geochim. Cosmochim. Acta **78**, 1–17 (2012).

R. H. Jones, "Petrology and mineralogy of type-II, FeO-rich chondrules in Semarkona (LL3.0)—origin by closed-system fractional crystallization, with evidence for supercooling," Geochim. Cosmochim. Acta **54**, 1785–1802 (1990).

S. A. Kirillova, V. I. Al'myashev, and V. V. Gusarov, "Spinodal breakdown in the SiO_2–TiO_2 system and formation of hierarchically arranged nanostructures," Nanosyst.: Fiz., Khim., Mathem. **3** (2), 100–115(2012).

R. J. Kirkpatrick, B. H. Reck, I. Z.Pelly, and Lung-Chuan Kuo, "Programmed cooling experiments in the system MgO–SiO_2: kinetics of a peritectic reaction," Am. Mineral. **68**, 1095–1101 (1983).

G. Kurat, C. Koeberl, T. Presper, F. Brandstatter, and M. Maurette, "Petrology and geochemistry of Antarctic micrometeorites," Geochim. Cosmochim. Acta **58**, 3879–3904 (1994).

D. S. Laurette, H. Nagahara, and C. M. O'D. Alexander, "Petrology and origin of ferromagnesian silicate chondrules," in *Meteorites and the Early Solar System II*, Ed. by D. S. Laurette and H. Y. McSween (Univ. of Arizona Press, 2006), pp. 431–459.

S. G. Love and D. E. Brownlee, "Heating and thermal transformation of micrometeoroids entering the Earth's atmosphere," Icarus **89**, 26–43 (1991).

S. G. Love and D. E. Brownlee "A direct measurement of the terrestrial mass accretion rate of cosmic dust," Science **262**, 550–553 (1993).

M. Maurette, C. Olinger, M. C. Mishel-Levy, G. Kurat, M. Pourchet, F. Brandstatter, and M. Bourot-Denise, "A collection of diverse micrometeorites recovered from 100 tonns of Antarctic blue ice," Nature **351**, 44–46 (1991).

H. D. Palme, C. Hezel, and D. S. Ebel, "The origin of chondrules: constraints from matrix composition and matrix–chondrule complementarity," Earth Planet. Sci. Lett. **411**, 11–19 (2015).

K. M. Parashar, S. Prasad, and S. S. Chauhan. "Investigation on a large collection of cosmic dust from the central Indian Ocean," Earth Moon Planets **107**, 197–217 (2010).

P. Rochette, L. Folco, C. Suavet, M. van Ginneken, J. Gattacceca, N. Perchiazzi, R. Braucher, and R. P. Harvey, "Micrometeorites from the Transantarctic Mountains," PNAS **105**, 18206–18211 (2008).

Taylor S. and Brownlee, D. E. "Cosmic spherules in the geologic record," Meteoritics **26**, 203–211 (1991).

S. Taylor, C. M. O. Alexander, J. S. Delaney, P. Ma, G. F. Herzog, and C. Engrand, "Isotopic fractionation of iron, potassium, and oxygen in stony cosmic spherules: implications for heating histories and sources," Geochim. Cosmochim. Acta **69**, 2647–2662 (2005).

S. Taylor, J. H. Lever, and R. P. Harvey, "Numbers, types, and compositions of an unbiased collection of cosmic spherules," Meteorit. Planet. Sci. **35**, 651–666 (2000).

I. V. Veksler, A. M. Dorfman, D. Rhede, R. Wirth, A. A. Borisov, and D. B. Dingwell, "Liquid unmixing kinetics and the extent of immiscibility in the system K_2O–CaO–FeO–Al_2O_3–SiO_2," J. Geol. **256**, 119–130 (2008).

T. Yada and H. Kojima, "The collection of micrometeorites collected in the Yamato Meteorite Ice Field of Antarctica in 1998," Antarct. Meteorit. Res. **13**, 9–18 (2000).

T. Yada, T. Nakamura, T. Noguchi, N. Matsumoto, M. Kusakabe, H. Hiyagon, T. Ushikubo, N. Sugiura, H. Kojima, and N. Takaoka, "Oxygen isotopic and chemical compositions of cosmic spherules collected from the Antarctic ice sheet: implications for their precursor material," Geochim. Cosmochim. Acta **69**, 5789–5804 (2005).

Translated by E. Kurdyukov